



## Original article

## Functional and morphological preservation of adult ventricular myocytes in culture by sub-micromolar cytochalasin D supplement

Qinghai Tian<sup>a,b,1</sup>, Sara Pahlavan<sup>a,b,1</sup>, Katharina Oleinikow<sup>a,c</sup>, Jennifer Jung<sup>a,c</sup>, Sandra Ruppenthal<sup>a,b</sup>, Anke Scholz<sup>a,b</sup>, Christian Schumann<sup>d</sup>, Annette Kraegeloh<sup>d</sup>, Martin Oberhofer<sup>a,b</sup>, Peter Lipp<sup>a,b,\*</sup>, Lars Kaestner<sup>a,b,\*</sup>

<sup>a</sup> Institute for Molecular Cell Biology, Medical Faculty, Building 61, Saarland University, 66421 Homburg/Saar, Germany

<sup>b</sup> Research Center for Molecular Imaging and Screening, Building 61, Saarland University, 66421 Homburg/Saar, Germany

<sup>c</sup> University of Applied Science, Campus Zweibrücken, Amerikastr. 1, 66428 Zweibrücken, Germany

<sup>d</sup> Leibniz-Institute for New Materials gGmbH, Campus D2, 66123 Saarbrücken, Germany

## ARTICLE INFO

## Article history:

Received 16 February 2011

Received in revised form 4 August 2011

Accepted 1 September 2011

Available online 10 September 2011

## Keywords:

Cytochalasin-D

Ventricular myocyte

Cell culture

Actin

T-tubules

Single cell model

STED microscopy

## ABSTRACT

In cardiac myocytes, cytochalasin D (CytoD) was reported to act as an actin disruptor and mechanical uncoupler. Using confocal and super-resolution STED microscopy, we show that CytoD preserves the actin filament architecture of adult rat ventricular myocytes in culture. Five hundred nanomolar CytoD was the optimal concentration to achieve both preservation of the T-tubular structure during culture periods of 3 days and conservation of major functional characteristics such as action potentials, calcium transients and, importantly, the contractile properties of single myocytes. Therefore, we conclude that the addition of CytoD to the culture of adult cardiac myocytes can indeed be used to generate a solid single-cell model that preserves both morphology and function of freshly isolated cells. Moreover, we reveal a putative link between cytoskeletal and T-tubular remodeling. In the absence of CytoD, we observed a loss of T-tubules that led to significant dys-synchronous  $\text{Ca}^{2+}$ -induced  $\text{Ca}^{2+}$  release (CICR), while in the presence of 0.5  $\mu\text{M}$  CytoD, T-tubules and homogeneous CICR were majorly preserved. Such data suggested a possible link between the actin cytoskeleton, T-tubules and synchronous, reliable excitation–contraction–coupling. Thus, T-tubular re-organization in cell culture sheds some additional light onto similar processes found during many cardiac diseases and might link cytoskeletal alterations to changes in subcellular  $\text{Ca}^{2+}$  signaling revealed under such pathophysiological conditions.

© 2011 Elsevier Ltd. All rights reserved.

### 1. Introduction

Cytochalasin D (CytoD) is a fungal metabolite that suppresses cyto-kinesis by blocking the formation of contractile microfilament structures and causes multinucleated cell formation, reversible inhibition of cell movement and the induction of cellular extrusion [1].

In cardiac myocytes, it is believed to act as a F-actin disruptor [2–6]. In such studies, CytoD was used beside diacetyl monoxime (DAM) and butanedione monoxime (BDM), which acts as a mechanical uncoupler on the organ level [5], in tissue [2,3] and with isolated myocytes [6]. However, other reports suggested that in adult ventricular myocytes CytoD stabilizes the actin cytoskeleton [7,8]. These studies indicated a

positive effect of CytoD on the morphology of cardiomyocytes using 40  $\mu\text{M}$  CytoD as a cell culture supplement.

The aim of the current study was to investigate how CytoD affects the morphology and function of adult cardiomyocytes in culture and whether and how CytoD can be used as a routine supplement in single cell models of cardiomyocytes.

We based our investigation on a previously optimized serum-free culture method of rat ventricular myocytes [9]. The major characteristics were the following: (i) a robust isolation procedure using a well-defined blend of digestion enzymes [10]; (ii) coating of the coverslips with a mixture of extracellular matrix proteins; and (iii) the addition of culture medium supplements including insulin, transferrin and selenite (ITS). We recently characterized this model further and found a gradual loss of T-tubular membranes during a culture period of 6 days *in vitro* (DIV) by a process referred to as “sequential pinching off”, from inside to outside [11]. We speculate that T-tubular remodeling and structural changes in the cytoskeleton might be related to each other. Such a mechanism would be of particular interest

\* Corresponding authors at: Institute for Molecular Cell Biology, Medical Faculty, Building 61, Saarland University, 66421 Homburg/Saar, Germany. Tel.: +49 6841 1626103; fax: +49 6841 1626104.

E-mail addresses: [peter.lipp@uks.eu](mailto:peter.lipp@uks.eu) (P. Lipp), [lars\\_kaestner@me.com](mailto:lars_kaestner@me.com) (L. Kaestner).

<sup>1</sup> These authors contributed equally.

because a number of relevant pathologies, particularly the development of heart failure, have recently been associated with T-tubular remodeling [12–14].

## 2. Material and methods

### 2.1. Cell isolation and culture

Ventricular myocytes were isolated from male Wistar rats and cultured as previously described [10]. CytoD (Sigma-Aldrich, Taufkirchen, Germany) was added to the culture medium at the concentrations indicated and was exclusively present when cells were in culture, i.e., during all acute measurements, CytoD was absent.

### 2.2. 3D imaging, STED and line scans

For 3D visualization of the plasma membrane, cells were stained with di-8-ANEPPS (Invitrogen, Darmstadt, Germany) and optically sectioned (0.2  $\mu\text{m}$  step size) on a TCS SP5 II (Leica, Mannheim, Germany) followed by deconvolution and 3D rendering as described [15].

Actin was visualized in cells that were chemically fixed at the indicated time points after cell isolation. To visualize the plasma membrane in the fixed cells, cardiomyocytes were transduced with an adenovirus (multiplicity of infection of 20) coding for a GPI-anchor coupled to YFP as described [11]. Actin was stained with phalloidin coupled to ATTO-647N (Atto-Tec GmbH, Siegen, Germany).

Cells were fixed in 4% paraformaldehyde (in PBS) for 10 min, washed in PBS and permeabilized in 0.5% Triton X-100 (in PBS) for 10 min. Samples were then blocked during a 20-min incubation in 5% bovine serum albumin (in PBS). Thereafter, they were treated with 0.5  $\mu\text{M}$  ATTO-647N phalloidin (2 hours at room temperature), washed with PBS, mounted in ProLong® Gold antifade reagent (Invitrogen) and stored at 4 °C until visualization.

Super-resolution imaging was performed on a TCS SP5 STED with an HCX Plan APO 100 $\times$ , 1.4 objective (Leica). For an initial overview of the actin (ATTO-647N phalloidin) and membrane labeling (GPI-YFP), we used the microscope's conventional confocal mode (excitation: 635 nm and 488 nm laser lines, respectively). Emissions were collected in the spectral range of 648–700 nm (ATTO dye) and 495–594 nm (YFP). For the merge of the despeckled images, the individual intensity was adjusted, and a red and green lookup-table was applied in ImageJ (Wayne Rasband, NIH, Bethesda, USA). A rescan of the actin staining at higher magnification was performed in the microscope's STED (stimulated emission depletion) mode. While the probe was excited with a ps pulsed 635 nm laser (PDL800-B, PicoQuant GmbH, Berlin, Germany), stimulated emission was induced by a fs-laser (Mai-Tai, Newport Corp., Irvine, USA). STED images were deconvolved by custom-made algorithms based on a linear Tikhonov-deconvolution implemented in MatLab (MathWorks, Ismaning, Germany).

Fast line scans were performed on Fluo-4-loaded myocytes as described previously [16]. The effective acquisition speed of the resonant scanner (TCS SP5 II, Leica) was 1000 lines per second, and the analysis of the line scans was performed as described [17].

### 2.3. Functional measurements, power spectral analysis and data statistics

Action potentials (AP) were measured in the whole-cell configuration of the patch-clamp technique as described previously [15].  $\text{Ca}^{2+}$  imaging was performed as previously published for mouse cardiomyocytes [18]. We evaluated the contractile performance of the myocytes by sarcomere length measurements as described before [19].

In statistical graphs, if Gaussian distributed, values are given as mean  $\pm$  SEM, if not Gaussian distributed values are presented in box plots presenting the median and 10% percentile. The number of

measurements is given in the format  $n=x/y$  with  $x$ =number of cells and  $y$ =number of animals.

The power spectral analysis of the T-tubular membrane system was performed as described previously [9,11]. For the analysis of the actin cytoskeleton, line profiles (5 pixels wide) were generated on parts of the cell that presented fairly straight sections of the actin bundles. These intensity profiles were Fourier transformed and the real component (power) was plotted against the spatial frequency. Finally, these power spectra were normalized to the baseline low frequency to the right of the characteristic peak between 0.5 and 0.7  $\mu\text{m}^{-1}$ , the maximum of which was used for statistical analysis.

Statistical significance was tested in Prism5 (GraphPad Software, La Jolla, USA) with unpaired t-tests. For those data without a Gaussian distribution, a nonparametric t-test (Mann–Whitney) was used. When data were significantly different, they were labeled as follows:  $p<0.05$  (\*),  $p<0.01$  (\*\*),  $p<0.001$  (\*\*\*)

## 3. Results

Based on reports of the beneficial effect of CytoD on the culture of cardiomyocytes [7,8] we applied CytoD in the suggested concentration of 40  $\mu\text{M}$  as a supplement to our optimized culture conditions [9,11]. In an initial series of experiments, we evaluated the CytoD effect on the morphology, basic  $\text{Ca}^{2+}$  handling and AP characteristics, the results of which are summarized in Fig. 1. Recently, we have reported that T-tubules disappear over a period of 3 days *in vitro* (DIV3) by pinching off from inside to outside [11]. The result of this process, also depicted in Fig. 1Aa (DIV3, Ctrl), was a detectable loss of membrane capacitance (Fig. 1Ab, black columns). In the continuous presence of 40  $\mu\text{M}$  CytoD in the culture medium, both membrane capacitance (Fig. 1Ab, red columns) and membrane morphology (Fig. 1Aa, DIV3, 40  $\mu\text{M}$  CytoD) appeared to be well retained. However, a closer analysis revealed that the T-tubular orientation was altered significantly from a regularly ordered arrangement at DIV0 to a high density, disordered distribution (cp. Fig. 1A, top row of panels). Moreover, functional parameters such as steady state  $\text{Ca}^{2+}$  transients (Fig. 1B) and action potentials (Fig. 1C) were largely altered in the continuous presence of 40  $\mu\text{M}$  CytoD. These data strongly suggested major modulatory and unfavorable effects of CytoD on all functional parameters investigated.

We therefore aimed to explore the possibility of whether CytoD could be applied in a concentration that would retain its positive effect on the conserved morphology but would not display functional impairments. For initial screening we analyzed dose-dependent changes in the amplitude of electrically induced  $\text{Ca}^{2+}$  transients (see Fig. 2A). As depicted in Fig. 2A, we performed the experiments at various CytoD concentrations (up to 3.6  $\mu\text{M}$ ) up to DIV3. This period was recently identified as sufficient for expression of exogenous proteins by adenoviral gene transfer [11,20]. The intersection between the DIV3 and DIV0 relationship thus indicated the most appropriate CytoD concentration (0.5  $\mu\text{M}$ ) for preserving the DIV0 behavior. Panels 2Ab–d compare the amplitude of typical transients (left column) and the kinetic properties after normalization (right column). In the following, we investigated whether additional important properties, including  $\text{Ca}^{2+}$  handling (Figs. 2B and 3), AP (Fig. 4), and contractility (Fig. 5), were also well preserved at this CytoD concentration.

Global  $\text{Ca}^{2+}$  handling was analyzed in greater detail with a post-rest behavior protocol stimulation as depicted in Fig. 2B. After a resting period, the first as well as the steady state amplitude of electrically-induced  $\text{Ca}^{2+}$  transients displayed a significant drop at DIV3 when compared to DIV0. In the presence of 0.5  $\mu\text{M}$  CytoD in the culture medium, such properties were preserved at typical levels for DIV0 (compare black and open columns in Figs. 2Ca and b, DIV3). When we analyzed the  $\text{Ca}^{2+}$  transient duration, we found that 0.5  $\mu\text{M}$  CytoD caused a prolongation as early as DIV0, but the massive prolongation observed during 3 days of culture without CytoD was

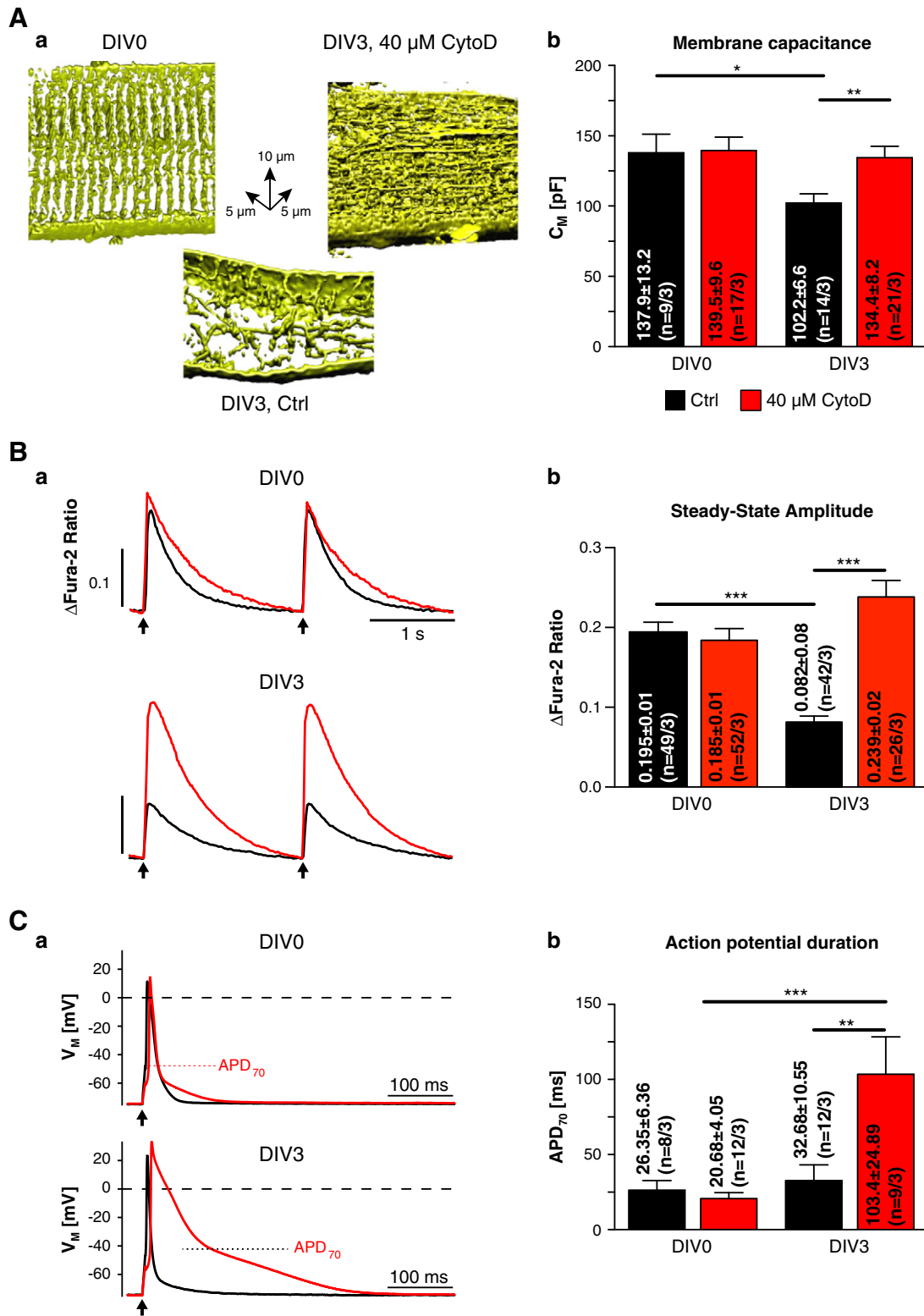


**Fig. 1.** Effects of 40  $\mu\text{M}$  CytoD on adult cultured rat ventricular myocytes. Panel (A) depicts changes in membrane topology. Representative 3D reconstructions of confocal sections at DIV0 and DIV3 with and without 40  $\mu\text{M}$  CytoD are plotted in (Aa), while (Ab) shows the statistical analysis of patch-clamp-based capacitance measurements under the conditions mentioned. Panel (B) reflects the  $\text{Ca}^{2+}$  handling under steady state conditions. (Ba) depicts examples of Fura-2 traces in cardiomyocytes at DIV0 and DIV3 with 40  $\mu\text{M}$  CytoD (red) and without CytoD (black), while (Bb) summarizes the statistics for the calcium transient amplitude. The black arrows in (Ba) indicate the time point of electrical field stimulation. Panel (C) compares the action potential at DIV0 and DIV3 with 40  $\mu\text{M}$  CytoD (red) and without CytoD (black) in representative examples (Ca) and the statistics of  $\text{APD}_{70}$  (Cb).

significantly reduced. In additional experiments, we further assessed characteristics of  $\text{Ca}^{2+}$  handling by discharging the sarcoplasmic reticulum (SR)- $\text{Ca}^{2+}$  store under steady state conditions (Fig. 3). For

this, we first electrically stimulated the cells and then in steady state briefly (5–10 s) applied 10 mM caffeine. For DIV3 cells treated with CytoD, we found that the amplitude (Fig. 3Bb) and the fractional

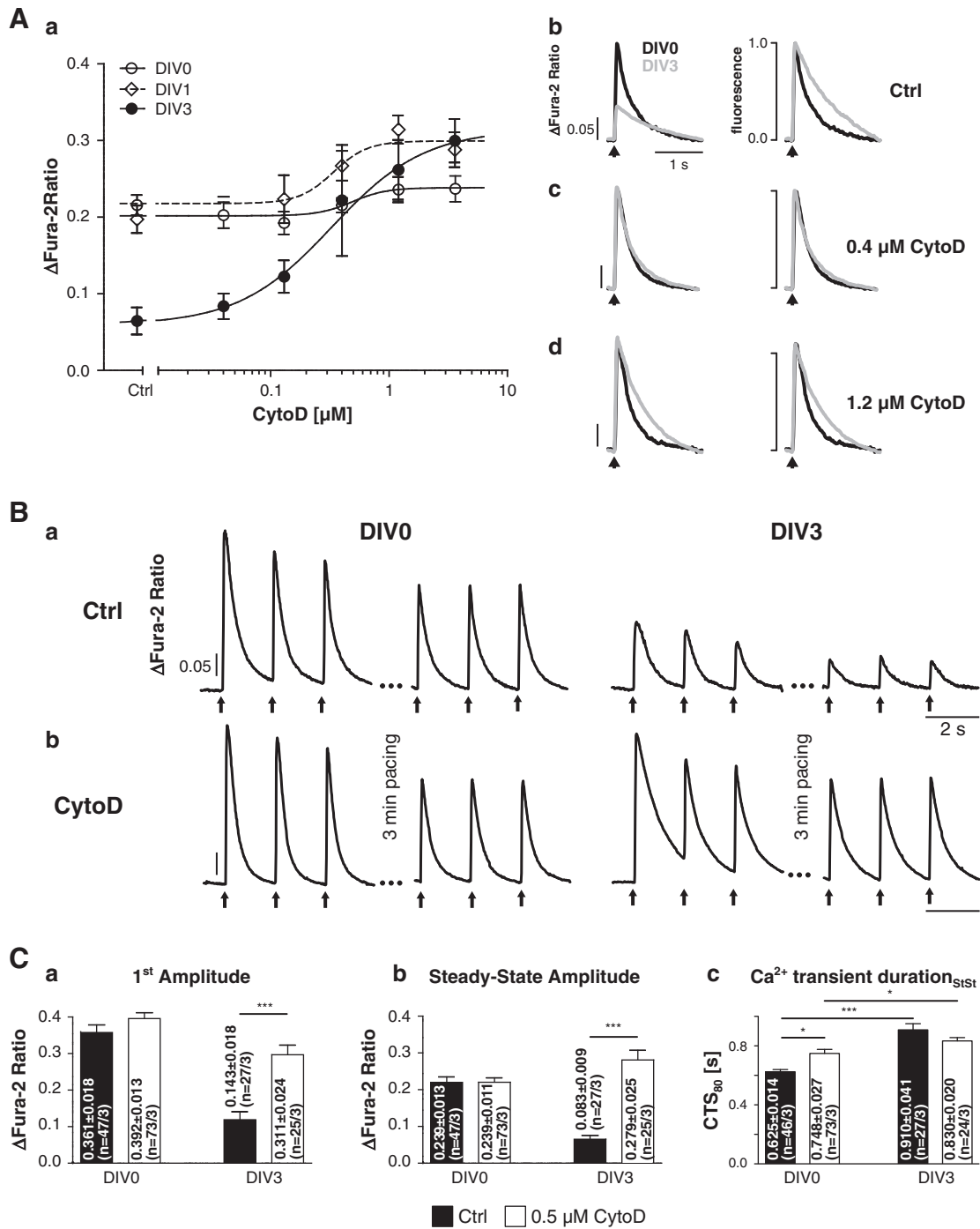


**Fig. 2.** Electrically evoked  $\text{Ca}^{2+}$  transients. Panel (Aa) depicts the dose–response curves for the given concentrations of CytoD at different days of culture (DIV0–DIV3). Panels (Ab–d) provide example traces for control conditions (Ab), for 0.4  $\mu\text{M}$  CytoD (Ac) and 1.2  $\mu\text{M}$  CytoD (Ad). The black arrows indicate the time point of electrical field stimulation. Panel (B) depicts a more detailed post-rest protocol to compare calcium transients in the presence and absence of 0.5  $\mu\text{M}$  CytoD in the culture medium at DIV0 and DIV3. Panel (Ba) depicts representative traces under control conditions and (Bb) in the presence of 0.5  $\mu\text{M}$  CytoD at both DIV0 and DIV3. The black arrows indicate the time point of electrical field stimulation. Panel (C) displays the statistical analysis of the Fura-2-based calcium amplitudes, namely the 1st amplitude after rest (Ca), the steady state amplitude (Cb) and the calcium transient duration (Cc).

$\text{Ca}^{2+}$  release (ratio of the  $\text{Ca}^{2+}$  transient amplitudes evoked by electrical stimulation over the transient amplitude induced by caffeine, Fig. 3Bc) resembled DIV0 values with CytoD, while the apparent NCX activity appeared to be slightly decreased (Fig. 3Bd).

Fig. 4 summarizes the properties of APs in the absence (black traces and columns) and in the continuous presence (gray traces, open columns) of 0.5  $\mu\text{M}$  CytoD in the culture medium. While without CytoD the AP amplitude displayed a significant drop at DIV3, the presence of 0.5  $\mu\text{M}$  CytoD prevented that effect, indicating that this concentration

resulted in good preservation of basic electrophysiological parameters (resting potential (Fig. 4Ba), AP amplitude (Fig. 4Bb) and APD (Fig. 4Bc–f)) over a culture time of 3 days.

Myocyte contractility was analyzed as electrically-induced changes of the sarcomere length (Fig. 5). After a resting period, the amplitude of the first contraction (Fig. 5Ba) as well as the steady state amplitudes (Fig. 5Bb) were decreased at DIV3 under control conditions. In the presence of 0.5  $\mu\text{M}$  CytoD, both parameters as well as the contraction duration (Figs. 5Bd and Be) were similar to

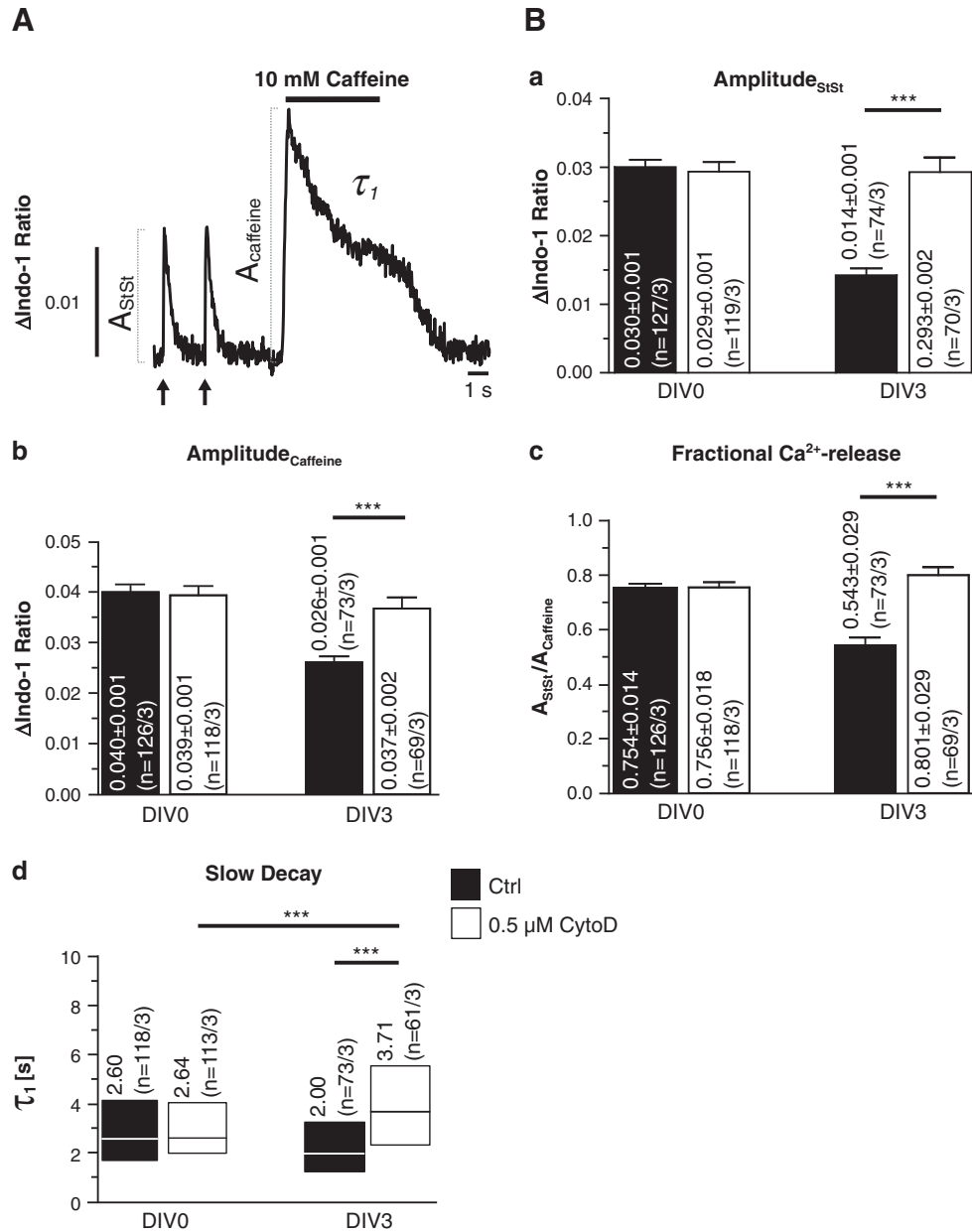


**Fig. 3.** Caffeine-induced  $\text{Ca}^{2+}$  release of rat ventricular myocytes with and without  $0.5 \mu\text{M}$  CytoD in the culture medium. Panel (A) plots an example trace under control conditions with all parameters indicated tested for statistical analysis (B). The black arrows below the traces indicate the time points of electrical stimulation, while the black bar above the trace represents the period of caffeine application. The following read-outs were analyzed: steady state amplitude (Ba), caffeine-induced amplitude (Bb), fractional  $\text{Ca}^{2+}$  release (Bc) calculated as the ratio of the former two parameters and the decay time constant (Bd) during caffeine application.

those found at DIV0. Thus, CytoD in the culture medium preserved the contractile properties.

Because reports regarding the interaction of CytoD and actin have been controversial (see Introduction) and CytoD is often referred to as a cytoskeleton disrupter, we decided to directly analyze the actin cytoskeleton by probing actin filaments with phalloidin. We performed high resolution and super resolution imaging of the resulting staining as summarized in Fig. 6. Fig. 6Aa displays a single confocal slice through a typical, freshly isolated myocyte with a representative fluorescence profile along the longitudinal axis (yellow line, Fig. 6Ba). Figs. 6Ab–d depict standard high-resolution confocal sections through typical cardiac myocytes labeled with phalloidin (red color) and GPI-YFP (green color). The latter staining was employed to indicate plasma membrane topology [11] in the same cell and to allow identification of structurally intact cells. Viral transduction was mandatory because standard membrane probes, such as those used for

Fig. 1A, did not withstand the permeabilization necessary for the application of the actin probe. Quantification of the actin staining was performed by analyzing the pattern of fluorescence along the longitudinal axis of the cells (yellow lines in Fig. 6A). The patterns displayed in Figs. 6Ba–d were quantified by power spectral analysis (Fig. 6Ca with color coding similar to Fig. 6B). Such analysis clearly indicated that without CytoD actin arrangement was already modulated as early as DIV1. For freshly isolated cells (DIV0, green line in Fig. 6Ca) and cells in  $0.5 \mu\text{M}$  and  $40 \mu\text{M}$  CytoD at DIV1 (Fig. 6Ca, gray and red line, respectively), the power spectrum shows similar peaks at the sarcomeric frequency ( $0.58 \mu\text{m}^{-1}$ ).

The diminished peak in the power spectrum for untreated myocytes at DIV1 (Fig. 6Ca, back line) indicated a loss of structure as a result of early remodeling processes. This observation was documented by results of a population analysis, as presented in Fig. 6Cb. This revealed a significant difference between untreated cells at DIV1 and all other conditions

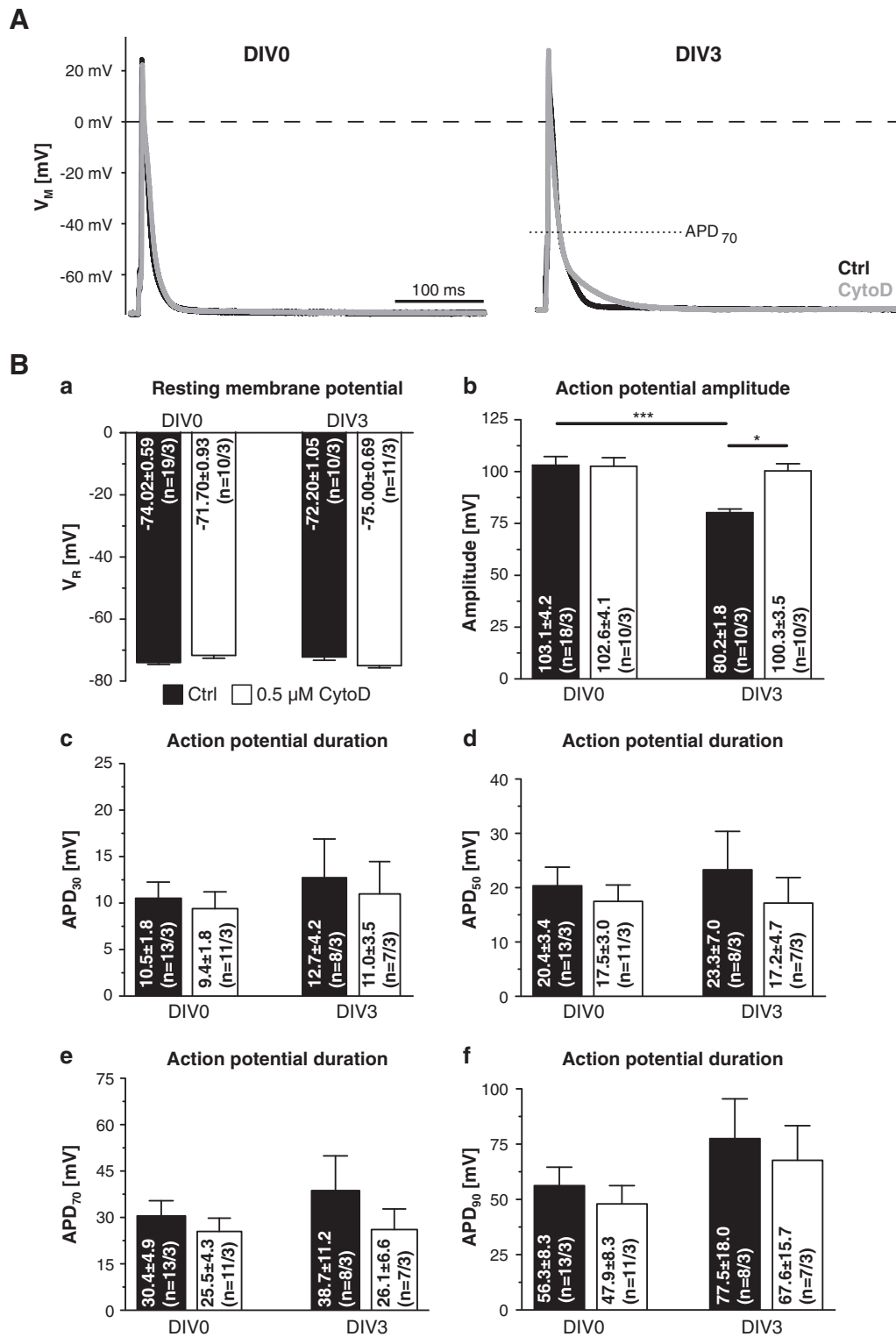


**Fig. 4.** Action potentials of rat ventricular myocytes with and without 0.5  $\mu$ M CytoD in the culture medium at DIV0 and DIV3. Panel (A) provides representative action potentials of the four conditions probed. Panel (B) shows the statistical analysis for the resting membrane potential (Ba), the action potential amplitude (Bb), the APD<sub>30</sub> (Bc), APD<sub>50</sub> (Bd), APD<sub>70</sub> (Be) and the APD<sub>90</sub> (Bf).

tested. We rescanned the regions marked by white boxes (Figs. 6Ab–d) at a higher magnification using STED imaging (Figs. 6Da–c) to enable easier identification of typical banding patterns. Thus, alterations in the cytoskeleton have already been identified as early as DIV1, at which time all cells displayed an unaltered T-tubular network (see green staining in Fig. 6A). In the presence of 0.5  $\mu$ M CytoD the analyzed properties of actin at DIV1 resembled those at DIV0.

In a further set of experiments, we addressed the question to what degree our optimized CytoD concentration modulated the remodeling of T-tubules during culture, e.g., DIV3 [11]. To that end, we probed the morphology of the plasma membrane with di-8-ANEPPS. The results are summarized in Fig. 7. The analysis of 3D surface renderings of typical cells suggested a conservation of T-tubular structures by 0.5  $\mu$ M CytoD (Fig. 7Aa). We quantified the images using power

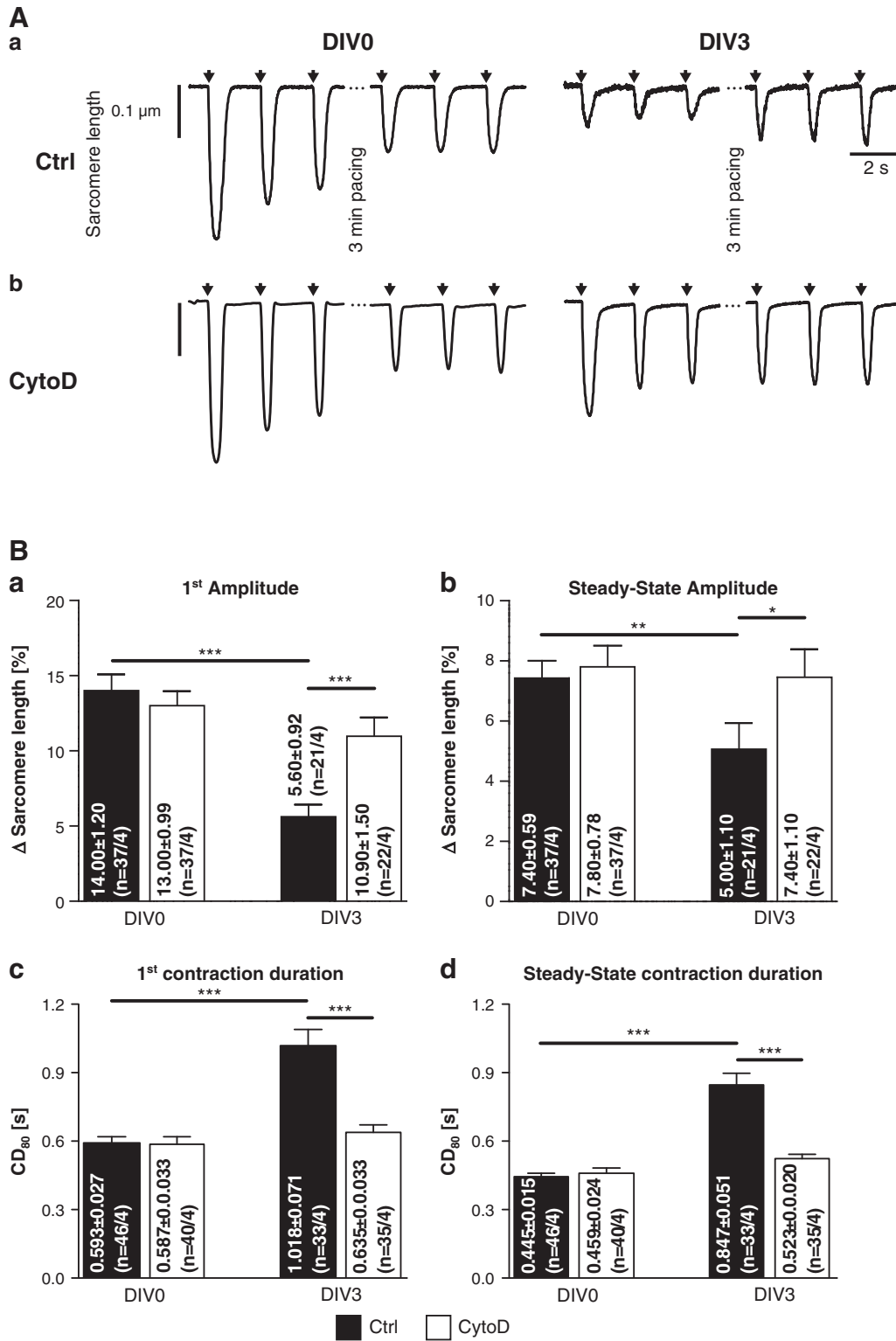


**Fig. 5.** Contraction of rat ventricular myocytes with and without 0.5 μM CytoD in the culture medium at DIV0 and DIV3. Panel (A) depicts representative sarcomere length measurements under control conditions (Aa) and in the presence of 0.5 μM CytoD (Ab) at both DIV0 and DIV3. The black arrows indicate the time points of electrical field stimulation. Panel (B) displays the statistical analysis for the first amplitude after rest (Ba), the steady state amplitude (Bb), the contraction duration D80 of the first contraction after rest (Bc) and in the steady state (Bd).

spectral analysis of the fluorescence distribution along the longitudinal axis of the myocytes (see dashed white lines in Fig. 7Aa) and found that the characteristic sarcomeric frequency peak at approximately 1.8 μm was much more prominent at DIV0 and DIV3 with 0.5 μM CytoD than at DIV3 without the supplement. We verified those results using a larger population of cells (Fig. 7Ba). To further

obtain additional independent support for our findings, we also employed electrophysiological characterization of the plasma membrane. We investigated the membrane capacitance of a population of myocytes and found that our optimized CytoD concentration also conserved DIV0 conditions of the membrane capacitance (compare DIV3 with DIV0 values in Fig. 7Bb).

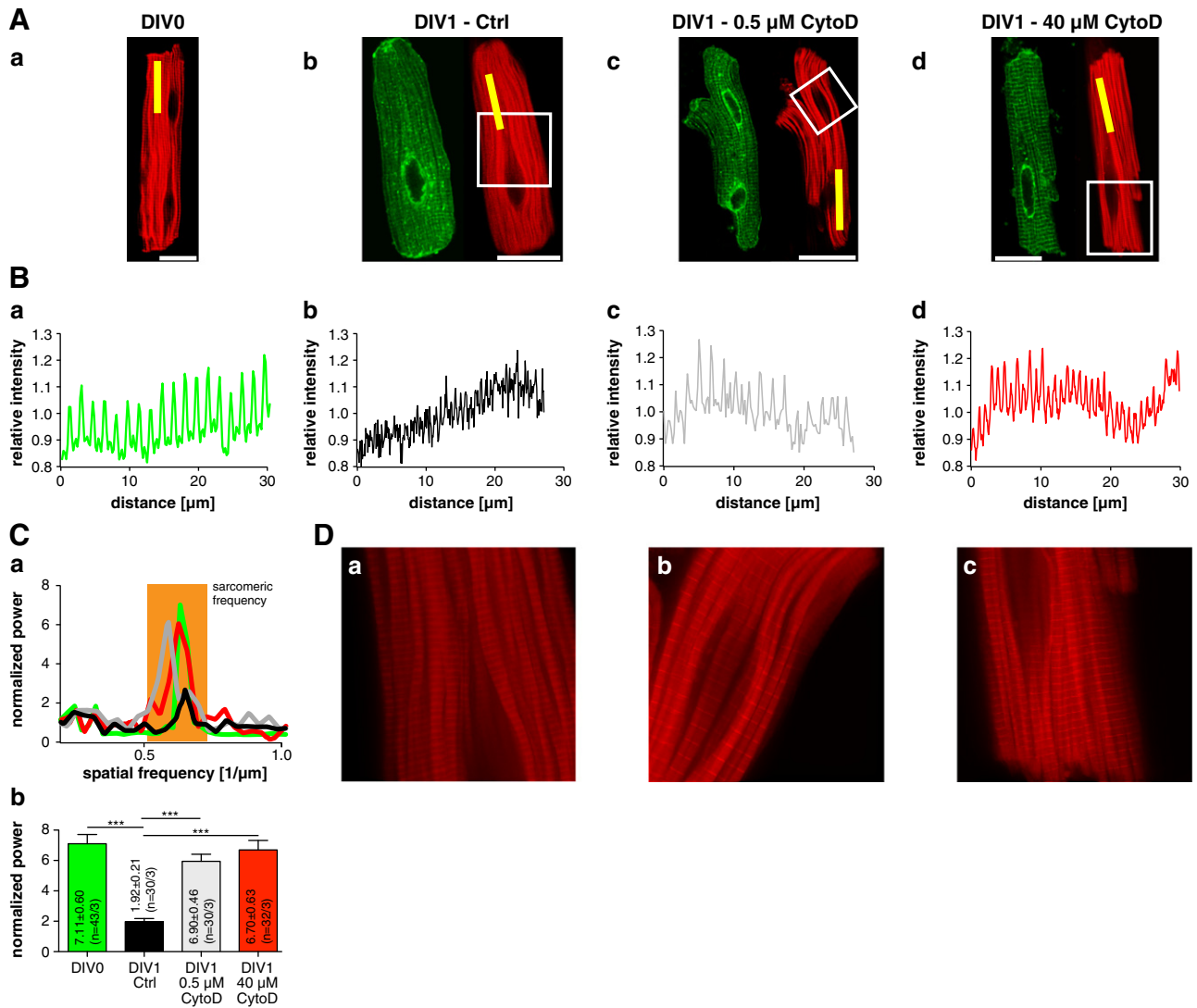


**Fig. 6.** Actin filaments in cultured adult rat ventricular myocytes. Representative images of rat cardiomyocytes expressing GPI-YFP as a membrane marker and stained by phalloidin-ATTO-647N to visualize the actin filaments. Cells are fixed at DIV0 (Aa) or DIV1 for all other conditions at different CytoD concentrations, as indicated above the image columns. The white bar in the confocal images (Aa)–(Ad) represents 20  $\mu\text{m}$ . The yellow bars indicate 2  $\mu\text{m}$ -wide stripes from which intensity profiles were taken and plotted below (Ba)–(Bd). Panel (Ca) depicts a power spectrum analysis of such profiles. The color code corresponds to the profiles in (Ba), (Bb) and (Bc). Panel (Cb) represents a statistical analysis of the normalized intensity of the power spectrum at the sarcomeric frequency. The subsections indicated by the white rectangle in (Ab), (Ac) and (Ad) were rescanned in the STED imaging mode and displayed in images (Da), (Db) and (Dc), respectively.

Finally, we were interested in the putative physiological consequences of preventing subcellular remodeling in the presence of CytoD and studied the subcellular properties of electrically evoked  $\text{Ca}^{2+}$  transients. For these experiments, we performed confocal line scans in the absence and the presence of 0.5  $\mu\text{M}$  and 40  $\mu\text{M}$  CytoD, as depicted in Fig. 8. In this study, DIV0 was compared to DIV3 and the statistical analysis also included the post-rest and the steady state behavior. Similar to a recent study [17], we also characterized the spatial properties of the  $\text{Ca}^{2+}$  transients by calculating the dyssynchrony index, that is, a quantitative measure of the transient's homogeneity during the upstroke period (see Figs. 8Ab–e). While the dyssynchrony index is a parameter that reflects the concerted action of the molecular players in CICR, the time to half amplitude is more indicative of the general coupling between calcium entry and calcium release. For both post-rest and steady state conditions, the dyssynchrony index at DIV3 was slightly increased in the presence of 0.5 and 40  $\mu\text{M}$  CytoD compared to DIV0 measurements but much less pronounced than in the absence of CytoD at DIV3.

When analyzing the time to half-amplitude (Figs. 8Bd–e), we found that while in the presence of 0.5  $\mu\text{M}$  cytoD, the values were unchanged between DIV0 and DIV3. Under all other conditions, this value was significantly altered. Thus, 0.5  $\mu\text{M}$  CytoD preserved the general coupling between  $\text{Ca}^{2+}$  influx and  $\text{Ca}^{2+}$  release and consequently maintained a robust EC coupling.

#### 4. Discussion

The current report represents a significant improvement in the culture conditions of adult ventricular myocytes to enable the conservation of both morphology and physiology. Moreover, it also provides initial evidence for possible mechanisms of T-tubular remodeling in general. Such alterations of the T-tubular characteristics have been described in various cardiac diseases, including the transition from hypertrophy to heart failure [13] and following myocardial infarction [17], but until now, no mechanistic insights

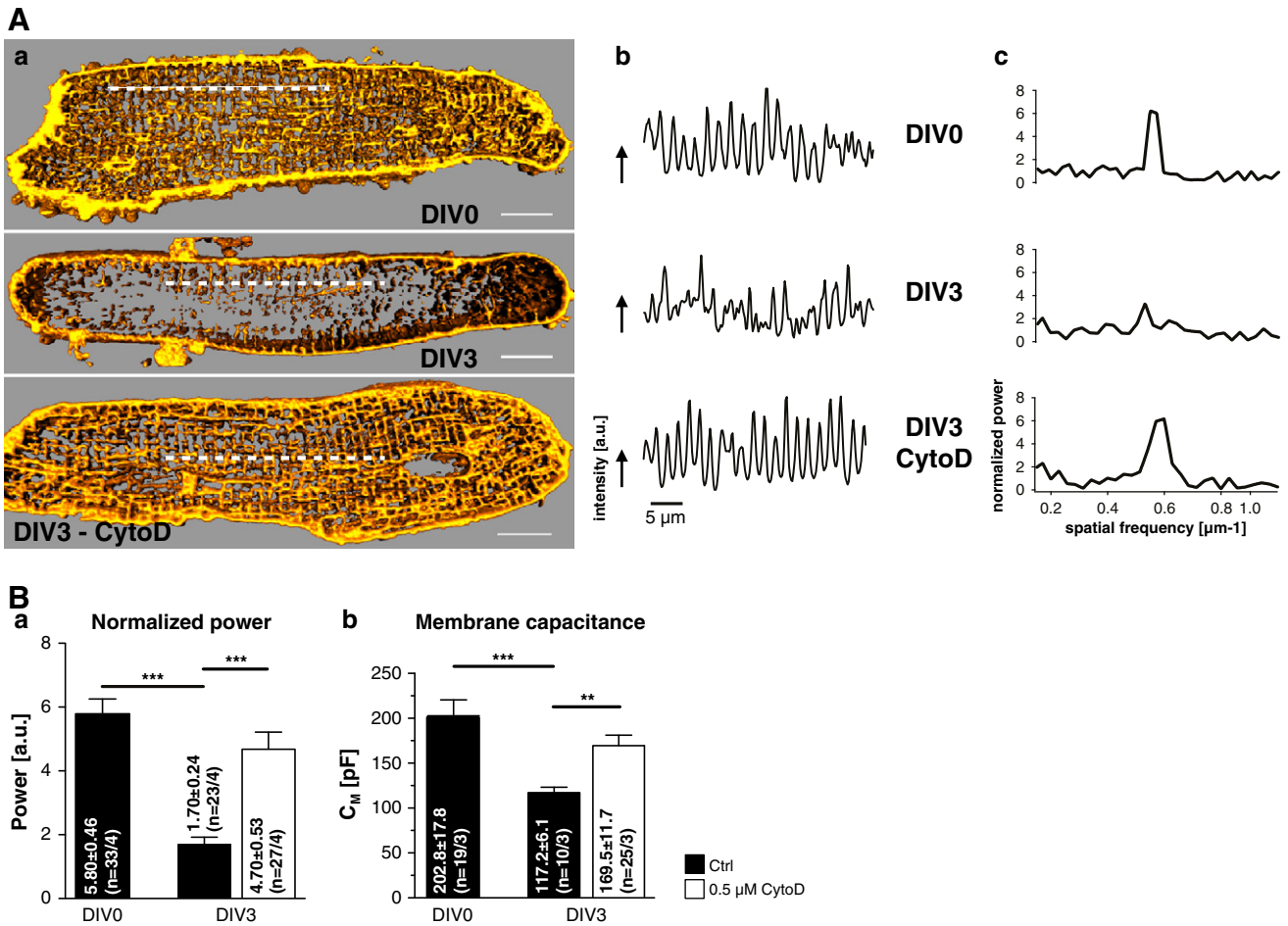


**Fig. 7.** T-tubular structure of rat ventricular myocytes with and without 0.5  $\mu\text{M}$  CytoD in the culture medium at DIV0 and DIV3. Panel (A) displays representative confocal sections of di-8-ANEPPS stained cells. (Aa) depicts 3D rendered cells that were cut open to reveal the T-tubular structure (DIV0 and DIV3 in the presence of 0.5  $\mu\text{M}$  CytoD) or the residues of the T-tubules (DIV3 in the absence of CytoD). (Ab) shows the corresponding intensity profile along the dashed white line in the images (Aa). From these, intensity profile power spectra were calculated and plotted in (Ac). Panel (Ba) summarizes the statistical analysis of such power spectra under the conditions given, while panel (Bb) depicts the corresponding patch-clamp-based capacitance measurements.

have been provided concerning how this plasma membrane remodeling might occur.

#### 4.1. Improved culture of adult cardiac myocytes

Our starting point was based on reports in which high CytoD concentrations not only disrupted excitation–contraction coupling but were also beneficial for long-term culture of adult cardiac myocytes [7,8]. We also found that 40  $\mu\text{M}$  CytoD diminished the loss of T-tubular structures, but we were left with initial doubts because the T-tubular arrangement was significantly altered. When compared to the DIV0 situation, we found T-tubular “crowding” (Fig. 1Aa). In a systematic approach, we set out to explore the potential of CytoD as a culture supplement by employing an important physiological parameter, i.e., the amplitude of electrically evoked  $\text{Ca}^{2+}$  transients, as an assay readout for dose–response relationships. The important result from these initial experiments was that CytoD at sub-micromolar concentrations preserved DIV0 conditions at DIV3 extremely well.

This initial notion was substantiated in additional studies investigating a plethora of physiological parameters, such as the post-rest behavior of electrically evoked global  $\text{Ca}^{2+}$  transients (Fig. 2B), SR- $\text{Ca}^{2+}$  content,  $\text{Ca}^{2+}$  removal mechanisms (Fig. 3), properties of action potentials (Fig. 4) and contractility (Fig. 5). The basic result of this experimental series was that CytoD at a concentration of 0.5  $\mu\text{M}$

prevented de-differentiation effects seen at DIV3, preserving structural and functional parameters found at DIV0. Despite a slight prolongation in calcium transient duration and an increase in NCX activity at DIV3 with 0.5  $\mu\text{M}$  CytoD, this treatment, to our knowledge, caused the best functional preservation reported after such a period *in vitro*. Interestingly, such a prolongation did not translate into extended contraction transients, as seen in Figs. 5Bc and Bd.

Reports on  $\text{Ca}^{2+}$  measurements in the presence of CytoD are rather sparse [7,21,22]. Although using 2-photon excitation recording of intracellular  $\text{Ca}^{2+}$  transients was successfully reported for Langendorff mouse hearts with 50  $\mu\text{M}$  CytoD, such transients could not be compared to control conditions because the mechanical uncoupling was a necessary requirement for these technically demanding experiments [21]. Leach et al. recorded line scans in the presence and absence of 40  $\mu\text{M}$  CytoD during a culture period of 4 days and described severe alterations in  $\text{Ca}^{2+}$  handling, but did not include a statistical/quantitative analysis [7]. In contrast to our current study, very often, acute effects of CytoD had been investigated, e.g., Howarth et al. reported such immediate effects using 40  $\mu\text{M}$  CytoD [22].

Under physiological  $\text{Na}^+$  concentrations, heterologously expressed NCX displayed 40% reduced activity with 1  $\mu\text{M}$  CytoD [23]. In ventricular myocytes, we did not find changes in the apparent NCX activity after 0.5  $\mu\text{M}$  CytoD treatment at DIV0, but a slight increase of the time constant  $\tau$  (decreased activity) at DIV3 was found.

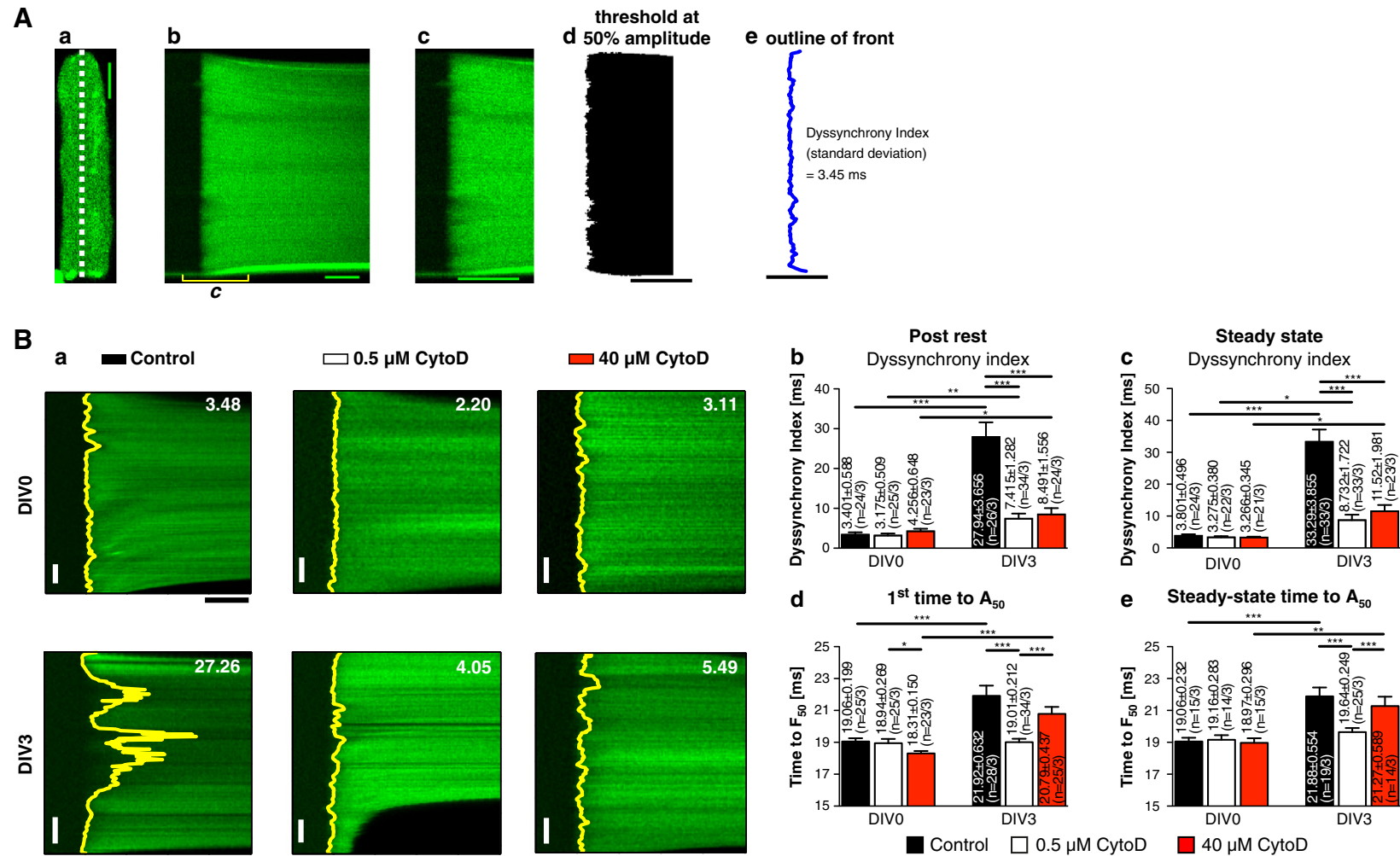


**Fig. 8.** CytoD effects on subcellular  $Ca^{2+}$  release. Panel (A) illustrates the procedure of data acquisition and analysis. In a 2D image of a cardiomyocyte, a line was chosen (Aa). The scale bar in (Ba) depicts 10  $\mu$ m. Along this line, a line scan was performed over time (Ab). Image (Ac) depicts a temporal enlargement to point out spatial differences in the calcium release. A binary image with the threshold of 50% amplitude is illustrated in (Ad). The standard deviation of the 50% line is defined as the dyssynchrony index (Ae). Typical line scans in the absence of CytoD, with 0.5  $\mu$ M CytoD and 40  $\mu$ M CytoD in the culture medium at DIV0 and DIV3 are plotted in (Ba). The yellow lines indicate the outline of the  $F_{50}$  profiles. The number in the top right corner denotes the dyssynchrony index of this particular line scan. The statistical analysis of the dyssynchrony index (Bb) and (Bc) as well as the time to 50% of the calcium amplitude (Bd) and (Be) under post-rest and steady state conditions, respectively, are shown. Throughout the line scans vertical scale bars depict 15  $\mu$ m and horizontal scale bars 50 ms.

Following acute application of 20–40  $\mu\text{M}$  and 10  $\mu\text{M}$  CytoD, previous investigations reported a 25% reduction in the  $\text{Na}^+$  current [4] and an abolishment of the  $\text{Ca}^{2+}$  mediated inward rectification of  $\text{K}^+$  channels [24], respectively. For alterations in both membrane currents, we would have expected a significant impact on the amplitude and shape (APD) of action potentials. Under our conditions, we could not find any changes in the shape of APs induced by the chronic treatment with 0.5  $\mu\text{M}$  CytoD. Nevertheless, our results are difficult to compare with previous reports because they all focused on acute CytoD effects. In our experiments, CytoD was only present in the culture medium but was washed out for the acute experiments. If there had been altered AP properties in the presence of CytoD, these effects would have been reversible immediately after washout.

In addition, the obvious differences in the functional parameters of the cardiac myocytes with CytoD treatment between our study and previous reports can most likely be explained by different concentrations of CytoD. While previous reports mainly used between 10 and 80  $\mu\text{M}$  CytoD [2,4,7,21,24], our culturing was performed at 0.5  $\mu\text{M}$  CytoD (Figs. 2B–5 and 7).

The action of CytoD on ventricular myocytes was clearly dose-dependent (Fig. 2A). We were particularly surprised by our finding that 0.5  $\mu\text{M}$  CytoD conserved the contractility of myocytes because CytoD was used as a mechanical uncoupler [2,3,5,6]. However, similar to above, we believe that this is a question of the concentration because a concentration of 4  $\mu\text{M}$  CytoD had no effect on the contraction in cat cardiomyocytes [25]. In addition, in Langendorff mouse hearts, 5  $\mu\text{M}$  CytoD was determined to be the minimum concentration that reliably reduced the developed pressure by more than 90% [5].

Based on this, we conclude that 0.5  $\mu\text{M}$  CytoD is the optimal concentration to maximally conserve cellular function over a culture period of at least 3 days. This is a sufficient time to enable the expression of fusion proteins and genetically encoded biosensors [9,11,20] and therefore can serve as an improved cellular model for genetic as well as pharmacological manipulations *in vitro*.

#### 4.2. The interplay of CytoD and actin

CytoD primarily acts on actin [26] and leads to mechanical uncoupling at a concentration of 40  $\mu\text{M}$  [4,6,21] but does not show mechanical uncoupling at concentrations of 0.5  $\mu\text{M}$  [5,25] (Fig. 5). To further investigate changes in the actin microarchitecture, we visualized the actin cytoskeleton in ventricular myocytes (Fig. 6). In all conditions studied, we surprisingly did not find a disruption of the actin arrangement. Initial reports on the interaction of CytoD and actin described binding of CytoD to the barbed end of actin filaments, thus preventing actin polymerization [27,28]. We believe that disruption and prevention of polymerization are not necessarily the same and that these interpretation differences contribute to the controversy found in the literature. Reports that focus on the molecular mechanism of CytoD action asserted that CytoD binding to actin prevented further polymerization/filament elongation by inducing net depolymerization [29–31]. Most likely, the binding of CytoD to actin together with its effect on mechanical uncoupling might have led to the concept of CytoD as an actin disruptor. Instead, Calaghan et al. suggested that mechanical uncoupling might be due to decreased myofilament sensitivity to  $\text{Ca}^{2+}$  through interaction with sarcomeric actin [6,32]. Therefore, we conclude that at the concentrations used in our report, CytoD leads to actin conservation rather than disruption.

We detected actin remodeling (more diffuse staining in Figs. 6Ab, Bb, Da) as early as after 1 day in culture and quantified that by power spectral analysis (Fig. 6C, black line and column). This cell culture-induced modulation was prevented with the optimized CytoD concentration identified in our current report. The addition of 0.5  $\mu\text{M}$  CytoD resulted in a conservation of actin filament banding (Figs. 6Ac, Bc, Db) very similar to the one found at DIV0 (Figs. 6Aa and Ba). Our power spectral analysis substantiated this notion (Fig. 6Cb, compare gray and

green columns). Due to the “freezing” of the actin filaments, the culture in the presence of CytoD excludes the study of actin filament dynamics in cardiomyocyte culture.

#### 4.3. CytoD as a pharmacological tool to study cardiomyocyte remodeling

As depicted in Figs. 2–5, the presence of 0.5  $\mu\text{M}$  CytoD in the culture medium conserved the functional properties of ventricular myocytes in culture. Although it was reported before that T-tubular remodeling could be prevented by high CytoD concentrations, our results strongly discourage the application of such high concentrations because in the current study, we found that 40  $\mu\text{M}$  CytoD, despite preventing T-tubular loss, clearly induced highly artificial T-tubular “crowding” (Fig. 1Aa). From this, we conclude that the application of 40  $\mu\text{M}$  CytoD substituted one kind of remodeling, i.e., loss of T-tubular structures, by another one, i.e., T-tubular “crowding”. Here, we present evidence that after “titration” of the CytoD concentration, one can find an optimal balance that resulted in a conservation of the regular cross-striational arrangement of T-tubules (see Fig. 7A).

As a culture supplement, 0.5  $\mu\text{M}$  CytoD prevented culture-dependent remodeling in all morphological and functional parameters that were analyzed. Culture-dependent alterations of functional properties can be primarily related to the loss of T-tubules and the resulting loss of L-type  $\text{Ca}^{2+}$  channel–RyR interactions. To provide further evidence for this assumption, we performed confocal line scans (Fig. 8). Here, we compared three different conditions: control medium and medium supplemented with either 0.5 or 40  $\mu\text{M}$  CytoD. To characterize the effects of the culture conditions on subcellular aspects of EC coupling, we analyzed rapid line scans during electrical stimulations by means of the following two different parameters: the dyssynchrony index (DI) and the time to half amplitude (Fig. 8). Notably, DI changed for all conditions when comparing DIV0 and DIV3. Nevertheless, the relative change was vastly different. While in the presence of CytoD, DI doubled, this value increased almost an order of magnitude without CytoD. When we analyzed EC coupling on a more global basis (time to half amplitude), both control as well as 40  $\mu\text{M}$  CytoD conditions showed alterations of this parameter, while our optimized concentration maintained DIV0 properties.

In summary, these findings suggest a possible link between remodeling of the cytoskeletal components and the observed T-tubular remodeling resulting in the appearance of orphaned RyR as in many cardiac diseases. It will thus be interesting to extend the findings and concepts described in the current report using cultured cardiac cells to mechanisms of plasma membrane remodeling observed, e.g., following myocardial infarction [17], in diabetic cardiomyopathy [33,34], during heart failure in general [12,14,35] or particularly during the transition from hypertrophy to heart failure [13]. We propose the short-term culture of adult ventricular myocytes (3 days to additionally allow virus-mediated genetic manipulation) as an appropriate model system to obtain additional insights into cellular structural remodeling during cardiac diseases.

#### Disclosures

None.

#### Acknowledgments

This work was supported by the following German institutions: the German Research Foundation (DFG–KFO196) and the Federal Ministry for Education and Research (BMBF). We would like to thank Anne Vecerdea for her excellent help in the cardiomyocyte isolation.

## References

- [1] Medical Subject Headings. US National Library of Medicine, Bethesda: U.S. National Institutes of Health; 2009.
- [2] Biermann M, Rubart M, Moreno A, Wu J, Josiah-Durant A, Zipes DP. Differential effects of cytochalasin D and 2,3 butanedione monoxime on isometric twitch force and transmembrane action potential in isolated ventricular muscle: implications for optical measurements of cardiac repolarization. *J Cardiovasc Electrophysiol* Dec 1998;9(12):1348–57.
- [3] Wu J, Biermann M, Rubart M, Zipes DP. Cytochalasin D as excitation–contraction uncoupler for optically mapping action potentials in wedges of ventricular myocardium. *J Cardiovasc Electrophysiol* Dec 1998;9(12):1336–47.
- [4] Undrovinas AI, Shander GS, Makielski JC. Cytoskeleton modulates gating of voltage-dependent sodium channel in heart. *Am J Physiol* Jul 1995;269(1 Pt 2):H203–14.
- [5] Baker LC, Wolk R, Choi BR, Watkins S, Plan P, Shah A, et al. Effects of mechanical uncouplers, diacetyl monoxime, and cytochalasin-D on the electrophysiology of perfused mouse hearts. *Am J Physiol Heart Circ Physiol* Oct 2004;287(4):H1771–9.
- [6] Calaghan SC, White E, Bedut S, Le Guennec JY. Cytochalasin D reduces  $Ca^{2+}$  sensitivity and maximum tension via interactions with myofilaments in skinned rat cardiac myocytes. *J Physiol* Dec 1 2000;529(Pt 2):405–11.
- [7] Leach RN, Desai JC, Orchard CH. Effect of cytoskeleton disruptors on L-type Ca channel distribution in rat ventricular myocytes. *Cell Calcium* Nov 2005;38(5):515–26.
- [8] Chung KY, Kang M, Walker JW. Contractile regulation by overexpressed ETA requires intact T tubules in adult rat ventricular myocytes. *Am J Physiol Heart Circ Physiol* May 2008;294(5):H2391–9.
- [9] Viero C, Kraushaar U, Ruppenthal S, Kaestner L, Lipp P. A primary culture system for sustained expression of a calcium sensor in preserved adult rat ventricular myocytes. *Cell Calcium* Jan 2008;43(1):59–71.
- [10] Kaestner L, Scholz A, Hammer K, Vecerde A, Ruppenthal S, Lipp P. Isolation and genetic manipulation of adult cardiac myocytes for confocal imaging. *J Vis Exp* 2009;31.
- [11] Hammer K, Ruppenthal S, Viero C, Scholz A, Edelmann L, Kaestner L, et al. Remodelling of  $Ca^{2+}$  handling organelles in adult rat ventricular myocytes during long term culture. *J Mol Cell Cardiol* Sep 2010;49(3):427–37.
- [12] Cannell MB, Crossman DJ, Soeller C. Effect of changes in action potential spike configuration, junctional sarcoplasmic reticulum micro-architecture and altered t-tubule structure in human heart failure. *J Muscle Res Cell Motil* 2006;27(5–7):297–306.
- [13] Wei S, Guo A, Chen B, Kutschke W, Xie YP, Zimmerman K, et al. T-tubule remodeling during transition from hypertrophy to heart failure. *Circ Res*. Aug 2010;107(4):520–31.
- [14] Lyon AR, MacLeod KT, Zhang Y, Garcia E, Kanda GK, Lab MJ, et al. Loss of T-tubules and other changes to surface topography in ventricular myocytes from failing human and rat heart. *Proc Natl Acad Sci U S A* Apr 21 2009;106(16):6854–9.
- [15] Tian Q, Oberhofer M, Ruppenthal S, Scholz A, Buschmann V, Tsutsui H, et al. Optical QT-screens based on adult ventricular myocytes. *Cell Physiol Biochem* Feb 21 2011;27:281–90.
- [16] Kaestner L, Lipp P. Non-linear and ultra high-speed imaging for explorations of the murine and human heart. In: Popp J, von Bally G, editors. *Optics in life science*. Munich: SPIE; 2007. 66330K-1–K-10.
- [17] Louch WE, Mork HK, Sexton J, Stromme TA, Laake P, Sjaastad I, et al. T-tubule disorganization and reduced synchrony of  $Ca^{2+}$  release in murine cardiomyocytes following myocardial infarction. *J Physiol* Jul 15 2006;574(Pt 2):519–33.
- [18] Reil JC, Hohl M, Oberhofer M, Kazakov A, Kaestner L, Mueller P, et al. Cardiac Rac1 overexpression in mice creates a substrate for atrial arrhythmias characterized by structural remodelling. *Cardiovasc Res* Aug 1 2010;87(3):485–93.
- [19] Muller O, Tian Q, Zantl R, Kahl V, Lipp P, Kaestner L. A system for optical high resolution screening of electrical excitable cells. *Cell Calcium* Mar 2010;47(3):224–33.
- [20] Kaestner L, Ruppenthal S, Schwarz S, Scholz A, Lipp P. Concepts for optical high content screens of excitable primary isolated cells for molecular imaging. In: Licha K, Lin CP, editors. *SPIE Biomedical Optics*; 2009. Munich: SPIE; 2009. p. 737–45.
- [21] Rubart M, Wang E, Dunn KW, Field LJ. Two-photon molecular excitation imaging of  $Ca^{2+}$  transients in Langendorff-perfused mouse hearts. *Am J Physiol Cell Physiol* Jun 2003;284(6):C1654–68.
- [22] Howarth FC, Boyett MR, White E. Rapid effects of cytochalasin-D on contraction and intracellular calcium in single rat ventricular myocytes. *Pflugers Arch* Oct 1998;436(5):804–6.
- [23] Reeves JP, Condrescu M, Chernaya G, Gardner JP.  $Na^{+}/Ca^{2+}$  antiporter in the mammalian heart. *J Exp Biol* Nov 1994;196:375–88.
- [24] Mazzanti M, Assandri R, Ferroni A, DiFrancesco D. Cytoskeletal control of rectification and expression of four substates in cardiac inward rectifier  $K^{+}$  channels. *FASEB J* Feb 1996;10(2):357–61.
- [25] Tsutsui H, Ishihara K, Cooper Gt. Cytoskeletal role in the contractile dysfunction of hypertrophied myocardium. *Science* Apr 30 1993;260(5108):682–7.
- [26] Ohmori H, Toyama S. Direct proof that the primary site of action of cytochalasin on cell motility processes is actin. *J Cell Biol* Feb 1992;116(4):933–41.
- [27] Brenner SL, Korn ED. Substoichiometric concentrations of cytochalasin D inhibit actin polymerization. Additional evidence for an F-actin treadmill. *J Biol Chem* Oct 25 1979;254(20):9982–5.
- [28] Brown SS, Spudich JA. Cytochalasin inhibits the rate of elongation of actin filament fragments. *J Cell Biol* Dec 1979;83(3):657–62.
- [29] Brown SS, Spudich JA. Mechanism of action of cytochalasin: evidence that it binds to actin filament ends. *J Cell Biol* Mar 1981;88(3):487–91.
- [30] Flanagan MD, Lin S. Cytochalasins block actin filament elongation by binding to high affinity sites associated with F-actin. *J Biol Chem* Feb 10 1980;255(3):835–8.
- [31] Morris A, Tannenbaum J. Cytochalasin D does not produce net depolymerization of actin filaments in HEp-2 cells. *Nature* Oct 16 1980;287(5783):637–9.
- [32] Calaghan SC, Le Guennec JY, White E. Cytoskeletal modulation of electrical and mechanical activity in cardiac myocytes. *Prog Biophys Mol Biol* Jan 2004;84(1):29–59.
- [33] Stolen TO, Hoydal MA, Kemi OJ, Catalucci D, Ceci M, Aasum E, et al. Interval training normalizes cardiomyocyte function, diastolic  $Ca^{2+}$  control, and SR  $Ca^{2+}$  release synchronicity in a mouse model of diabetic cardiomyopathy. *Circ Res* Sep 11 2009;105(6):527–36.
- [34] McGrath KF, Yuki A, Manaka Y, Tamaki H, Saito K, Takekura H. Morphological characteristics of cardiac calcium release units in animals with metabolic and circulatory disorders. *J Muscle Res Cell Motil* 2009;30(5–6):225–31.
- [35] Song LS, Sobie EA, McCulle S, Lederer WJ, Balke CW, Cheng H. Orphaned ryanodine receptors in the failing heart. *Proc Natl Acad Sci U S A* Mar 14 2006;103(11):4305–10.